

# APPARATUS AND DEMONSTRATION NOTES

The downloaded PDF for any Note in this section contains all the Notes in this section.

Frank L. H. Wolfs, *Editor*

*Department of Physics and Astronomy, University of Rochester, Rochester, New York 14627*

This department welcomes brief communications reporting new demonstrations, laboratory equipment, techniques, or materials of interest to teachers of physics. Notes on new applications of older apparatus, measurements supplementing data supplied by manufacturers, information which, while not new, is not generally known, procurement information, and news about apparatus under development may be suitable for publication in this section. Neither the *American Journal of Physics* nor the Editors assume responsibility for the correctness of the information presented.

Manuscripts should be submitted using the web-based system that can be accessed via the *American Journal of Physics* home page, <http://ajp.dickinson.edu> and will be forwarded to the ADN editor for consideration.

## Two-dimensional heat flow apparatus

Patrick McDougall<sup>a)</sup> and Eric Ayars

*Department of Physics, California State University, Chico*

(Received 1 August 2013; accepted 15 February 2014)

We have created an apparatus to quantitatively measure two-dimensional heat flow in a metal plate using a grid of temperature sensors read by a microcontroller. Real-time temperature data are collected from the microcontroller by a computer for comparison with a computational model of the heat equation. The microcontroller-based sensor array allows previously unavailable levels of precision at very low cost, and the combination of measurement and modeling makes for an excellent apparatus for the advanced undergraduate laboratory course. © 2014 American Association of Physics Teachers.

[<http://dx.doi.org/10.1119/1.4867053>]

### I. INTRODUCTION

Heat flow experiments at the undergraduate level are usually limited to the one-dimensional case. The most common experimental setup is to measure the temperature at multiple points along a copper pipe with fixed temperatures at the ends. With advances in microcontroller technology, it is possible to make significant improvements in both the precision and the dimensionality of this basic apparatus. For the apparatus presented here, we are measuring the temperature at one hundred discrete points located on a  $10 \times 10$  grid across the surface of a 30-cm-square aluminum plate, shown in Fig. 1. The temperature at each point is measured every 2 s,

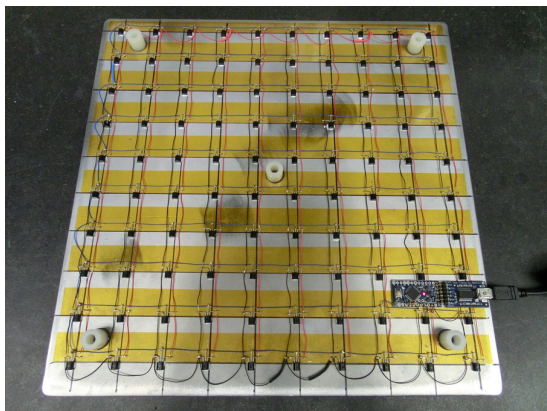


Fig. 1. The bottom of the completed 2-D heat plate apparatus, showing the 100 temperature sensors and the microcontroller.

and the resulting data can be compared with computational solutions of the heat flow equation.

The apparatus described can be built for less than \$300. The same technique can be adapted to many other sensor configurations such as odd geometries, an improved one-dimensional heat flow apparatus, or any situation in which it is desirable to measure temperature at a large number of points with high speed and precision.

### II. CONSTRUCTION

The key component to this apparatus is the Dallas Semiconductor DS18B20 temperature sensor. This device comes in a standard 3-pin TO-92 package and measures temperatures from  $-55^{\circ}\text{C}$  to  $+125^{\circ}\text{C}$  with either 9- or 12-bit precision. Rather than reporting temperature with an analog signal, these devices communicate via the “1-Wire” protocol. Every DS18B20 has a unique hard-coded address, and it is possible to place multiple sensors on a single bus and allow the control device to retrieve temperature measurements from individual sensors.<sup>1</sup>

The other component of the sensor network is the microcontroller. There are many options for the microcontroller, and we chose to use an Arduino microcontroller.<sup>2</sup> The Arduino is an open-source development board which includes power management, USB communications, and a user-friendly programming environment. Of the numerous types of Arduino microcontrollers available, we used the Arduino Pro Mini.<sup>3</sup>

The base of our apparatus was cut from a 6-mm thick aluminum plate. After cutting the plate square and thoroughly cleaning the surface, we glued 100 DS18B20 sensors on a

grid distributed across one face of the plate, using “Arctic Silver” thermal epoxy.<sup>4</sup> Strips of 18-mm Kapton tape were used as alignment guides and to provide insulation between the sensor leads and the plate. We then attached the microcontroller and ran power and ground wires from the controller to all of the sensors. The controller is powered via the USB connection to the computer.

Each DS18B20 temperature sensor has a unique address, but there is no external indication of what that address is. The microcontroller was programmed to determine these addresses by sending a command on the signal bus to request that all available temperature sensors report their addresses. The observed addresses were sent to the computer via the USB connection. We then temporarily connected each sensor, one at a time, to the control bus line and used the same program to create an address map of the sensor array. Once the address map was constructed, we permanently soldered the bus line to all sensors.

The final step in the construction of the apparatus was to program the microcontroller. This required two distinct steps. The first step was to write the address map to the non-volatile EEPROM on the microcontroller in a left-to-right, top-to-bottom order. The second step was to write the final “operating” program to the microcontroller. This program first sends out a signal on the bus to all sensors to record their temperature. It then pulls the first address from EEPROM and sends a command to the sensor at that address to report its observation. The reported temperature is sent via the USB connection to the computer, and the microcontroller then pulls the next address from EEPROM and repeats the process until it has polled all sensors. When all sensor temperatures have been obtained, the microcontroller repeats the process by once again sending commands to record the sensor temperatures. This continues indefinitely, as needed by the application.

All programs used by the microcontroller and the computer are available as supplementary material associated with this paper.<sup>5</sup>

### III. OPERATION

The completed apparatus sends each “frame” of temperature data as a single line of whitespace-delimited text. Frames are sent at approximately 2-s intervals. Serial data in this form can be read by any computer system, and there are many good choices of language for reading and displaying the data. We chose to use Python, but LabVIEW or C/C++ would be equally good choices. With our Python program, we can display the thermal data as a contour map while saving each frame for future analysis and comparison with theory.

By default, the temperature sensors are set to 9-bit precision, roughly 0.3 °C, and we left the device at that precision rather than switching to 12-bit, in order to keep the frame rate as high as possible. Figure 2 shows a typical frame, as rendered by our Python program.

### IV. THEORETICAL SETUP

The heat equation for an adiabatic system is given by

$$c_p \rho \frac{\partial T}{\partial t} - k \nabla^2(T) = 0, \quad (1)$$

where  $c_p$  is the heat capacity,  $\rho$  the mass density,  $k$  the thermal conductivity of the material being studied,  $T$  the

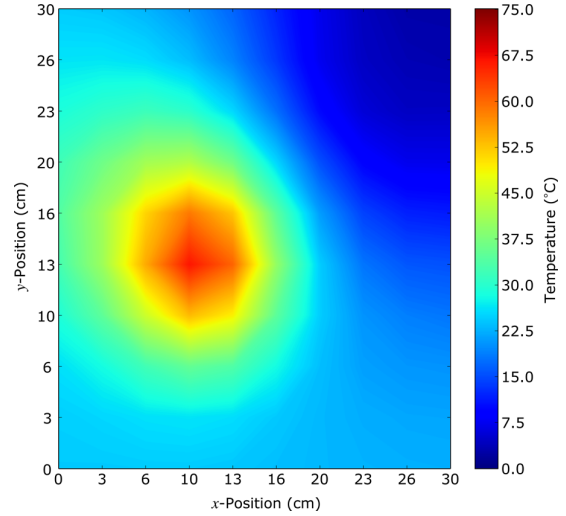


Fig. 2. A typical frame of data from the 2-D heat plate. This frame was obtained while holding a bag of crushed ice at the top right and a blow torch near the center.

temperature, and  $\partial/\partial t$  and  $\nabla$  represent the usual time and spatial derivatives. Because the temperatures involved are near the ambient room temperature and since aluminum has a very high thermal conductivity compared to the rate of heat transfer to the surrounding air, the adiabatic approximation is valid.

Since there is no general analytical solution to Eq. (1), we used the method of finite differences,

$$\frac{\partial T}{\partial t} \cong \frac{T_{i,j,n+1} - T_{i,j,n}}{\Delta t} \quad (2)$$

and

$$\nabla^2(T) \cong \frac{T_{i+1,j,n} - 2T_{i,j,n} + T_{i-1,j,n}}{(\Delta x)^2} + \frac{T_{i,j+1,n} - 2T_{i,j,n} + T_{i,j-1,n}}{(\Delta y)^2}, \quad (3)$$

where  $i$  represents the index of the  $x$  coordinate,  $j$  the index of the  $y$  coordinate, and  $n$  the time step. For our apparatus we have equal spatial steps in the  $x$  and  $y$  directions, so  $\Delta x = \Delta y$ . Solving for the next  $(n+1)$  temperature at some point  $(i, j)$ , we obtain

$$T_{i,j,n+1} = T_{i,j,n} + \frac{k\Delta t}{c_p \rho \Delta x^2} (T_{i+1,j,n} + T_{i,j+1,n} - 4T_{i,j,n} + T_{i-1,j,n} + T_{i,j-1,n}). \quad (4)$$

We replace the constants with a single constant,  $F_{0M} \equiv k\Delta t/(c_p \rho \Delta x^2)$ , commonly referred to as the Mesh Fourier Number.<sup>6</sup>

The geometrical and physical terms in  $F_{0M}$  are constrained by our experimental apparatus, and the value of  $F_{0M}$  determines the time step for the simulation. This replacement and a slight rearrangement of terms in Eq. (4) give

$$T_{i,j,n+1} = (1 - 4F_{0M})T_{i,j,n} + F_{0M}(T_{i+1,j,n} + T_{i,j+1,n} + T_{i-1,j,n} + T_{i,j-1,n}). \quad (5)$$

For stability in the computational model, the value of  $F_{OM}$  must be less than 0.25.

## V. BOUNDARY CONDITIONS AND INTEGRATION METHODS

Equation (5) is reminiscent of the relaxation method<sup>7</sup> in that the temperature at each step depends (in some sense) on the average temperature at the surrounding points in the previous step. Like the relaxation method, there is the question of what to do with boundary points. Recalling our earlier assumption that the system is adiabatic, we can set the heat flow from the boundary to zero. This condition is met if the material extends beyond the boundary and the temperature of those extended points is the same as the temperature at the boundary points. A zero temperature difference results in zero heat flow. For the sake of this calculation, we use “virtual points” just beyond the boundary, each at the temperature of the adjacent boundary point, or

$$T_{i,j_{\max}+1,n} = T_{i,j_{\max},n}. \quad (6)$$

The experimental setup uses an evenly spaced  $10 \times 10$  grid, where each sensor is separated by 2.9 cm. In order for the finite difference approximation to be accurate, both  $\Delta t$  and  $\Delta x$  should be small, with  $\Delta t$  set by choosing a Mesh Fourier Number, and  $\Delta x$  depends on the spacing of the experiment. However,  $\Delta x$  can be made smaller by creating a fine-scale grid for the simulation. We chose a  $100 \times 100$  simulation grid for the calculation, and used cubic interpolation to fill in the initial values of the simulation grid based on the values from the  $10 \times 10$  experimental grid.

Once this initial simulation grid was set, we applied Eq. (5) repeatedly, using the “virtual points” at the boundaries, to calculate the subsequent time evolution of the system. For the simulation grid chosen,  $\Delta x = 0.29$  cm and  $\Delta t = 0.0002$  s. Since the time and spatial step sizes for the simulation are not the same as the time and spatial steps for the experiment, we extracted the relevant points from the appropriate frames of the simulation to compare with the experimental data.

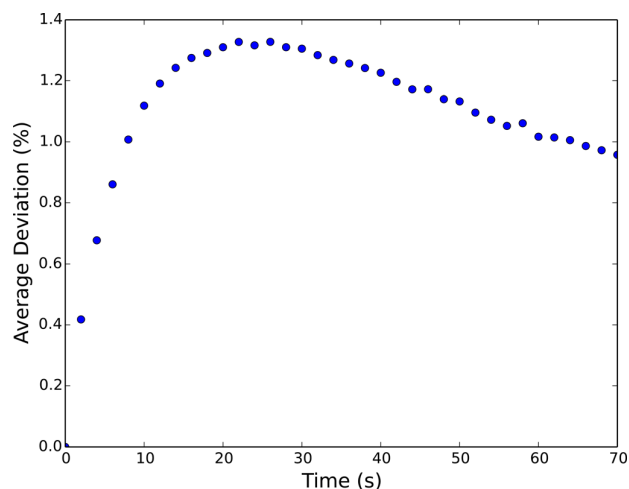


Fig. 3. The average deviation of our computational model from the experimental data as a function of time for a typical experimental run.

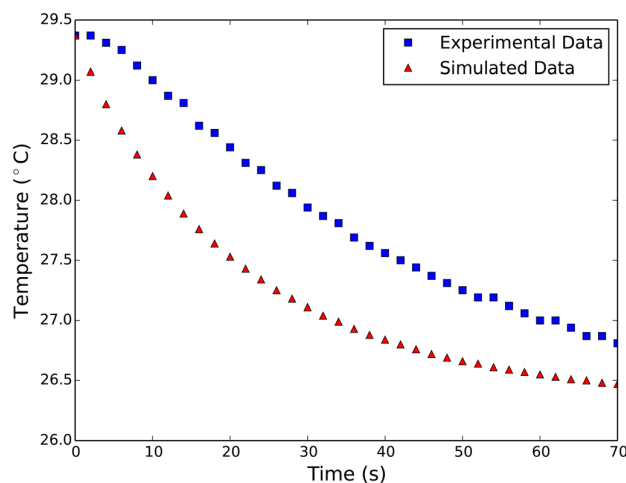


Fig. 4. The experimental and simulated temperature as a function of time near the center of the plate.

## VI. RESULTS AND LABORATORY USE

After the simulation is complete, its results can be compared to the experimental data. The comparison here was done for a Gaussian-like temperature profile that was achieved by placing a heat gun over the center of the device. We then removed the heat source and let the program collect data for about one minute. We compared the theoretical and experimental results in two ways. The first comparison we made was to look at the deviation between the measured and the calculated temperature at each point and average the magnitude of this deviation across the experimental grid. This average deviation is shown in Fig. 3 as function of time. The second comparison we made was to look at one common point near the center of our experiment and compare the measured and the simulated temperature as function of time. This comparison is shown in Fig. 4.

Our apparatus offers a distinct improvement over more traditional heat flow experiments in the advanced physics laboratory. In addition to the more interesting geometry, compared to the usual 1-D case, use of this apparatus presents an opportunity to provide students with a challenging but tractable computational modeling problem for comparison with experimental data. The sensitivity of the DS18B20 sensors allows useful experiments to be done at temperatures close to ambient temperatures, making it possible to use the adiabatic approximation without extensive insulation. The ability to monitor a large number of temperature sensors with a single microcontroller has the potential to be of use in many other laboratory applications.

## ACKNOWLEDGMENTS

The authors would like to thank Daniel Lund for his assistance in constructing this apparatus, particularly his diligence in determining the internal addresses of all 100 sensors.

<sup>a)</sup>Electronic mail: pmcdougall@mail.csuchico.edu

<sup>1</sup>There is no *theoretical* limit on the number of sensors that could be tied to the same bus. The available memory of the microcontroller and the cumulative current draw of all the sensors on the data line do provide a *practical* limit, however, and 100 sensors is approaching that limit.

<sup>2</sup>More information is available at <[www.arduino.cc/](http://www.arduino.cc/)>.

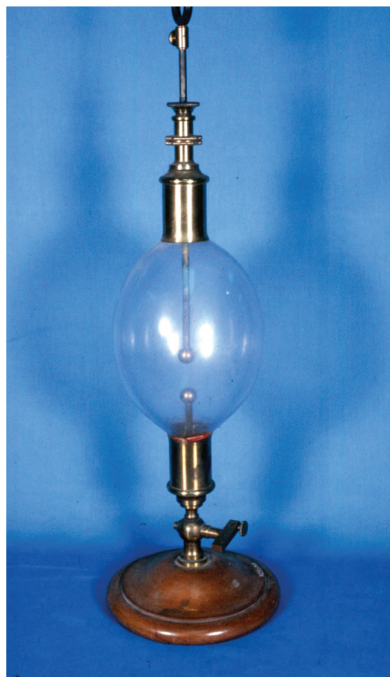
<sup>3</sup>Available at <[www.sparkfun.com/](http://www.sparkfun.com/)>.

<sup>4</sup>Available at computer supply and repair stores.

<sup>5</sup>See supplementary material containing all programs used for the microcontroller and simulation can be found at <http://dx.doi.org/10.1119/1.4867053>.

<sup>6</sup>Y. A. Cengel and A. J. Ghajar, *Heat and Mass Transfer: Fundamentals and Applications*, 4th ed. (McGraw-Hill, New York, 2011).

<sup>7</sup>M. DiStasio and W. C. McHarris, "Electrostatic problems? relax!," *Am. J. Phys.* **47**(5), 440–444 (1979).



### Electric Egg

This device allows the experimenter to investigate electrical discharges in a number of rarified gasses. A gas or liquid is introduced into the egg, and a mechanical pump used to exhaust the interior to the desired degree of rarefaction. A high-tension electric potential is set up between the electrodes using an induction coil, and the upper electrode is lowered until the discharge commences. It was bought from Ducretet of Paris in the mid-1880s to replace the collection of apparatus destroyed by fire at Amherst College. (Notes and photograph by Thomas B. Greenslade, Jr., Kenyon College)